



Tectonics, sea-level changes and palaeoenvironments in the early Pleistocene of Rome (Italy)

Domenico Cosentino^{a,*}, Paola Cipollari^a, Letizia Di Bella^b, Alessandra Esposito^c, Costanza Faranda^a, Guido Giordano^a, Elsa Gliozzi^{a,d}, Massimo Mattei^a, Ilaria Mazzini^d, Massimiliano Porreca^a, Renato Funicello^a

^a Dipartimento di Scienze Geologiche – Università degli Studi Roma Tre, L.go S. Leonardo Murialdo, 1, I-00146 Roma, Italy

^b Dipartimento di Scienze della Terra – Università degli Studi di Roma “La Sapienza”, P.le Aldo Moro, 5, I-00185 Roma, Italy

^c Istituto Nazionale di Geofisica e Vulcanologia, Via di Vigna Murata, 605, I-00143 Roma, Italy

^d IGAG CNR, Via Bologna, 7, I-00138 Roma, Italy

ARTICLE INFO

Article history:

Received 21 July 2007

Available online 17 May 2009

Keywords:

Stratigraphy

Sequence stratigraphy

Biostratigraphy

Paleoecology

Paleomagnetism

Tectonics

Plio-Pleistocene

Geology of urbanized areas

Central Italy

Rome

ABSTRACT

The historical site of the Monte Mario lower Pleistocene succession (Rome, Italy) is an important marker of the Pliocene/Pleistocene boundary. Recently, the Monte Mario site was excavated and restudied. A spectacular angular unconformity characterizes the contact between the Monte Vaticano and the Monte Mario formations, which marks the Pliocene/Pleistocene boundary. Biostratigraphical analyses carried out on ostracod, foraminifer, and calcareous nannofossil assemblages indicate an Early Pliocene age (topmost Zanclean, 3.81–3.70 Ma) for the underlying Monte Vaticano Formation, whereas the Monte Mario Formation has been dated as early Pleistocene (Santerian, 1.66–1.59 Ma). Palaeomagnetic analyses point to C2Ar and C1r2r polarity chrons for the Monte Vaticano and the Monte Mario formations, respectively. The Monte Mario Formation consists of two obliquity-forced depositional sequences (MM1 and MM2) characterized by transgressive systems tracts of littoral marine environments at depths, respectively, of 40–80 m and 15–20 m. The data obtained from foraminifer and ostracod assemblages allow us to reconstruct early Pleistocene relative sea-level changes near Rome. At the Plio/Pleistocene transition, a relative sea-level drop of at least 260 m occurred, as a result of both tectonic uplift of the central Tyrrhenian margin and glacio-eustatic changes linked to early Pleistocene glaciation (Marine Isotope Stage 58).

© 2009 University of Washington. Published by Elsevier Inc. All rights reserved.

Introduction

The Monte Mario succession has historically played a role in discussions about the definition of the global stratotype for the Pliocene/Pleistocene boundary. At the 18th International Geological Congress (London, 1948), the International Commission on Stratigraphy suggested that the Pliocene/Pleistocene boundary stratotype should be placed at the base of the Italian Calabrian stage, in accordance with the first indication of climatic deterioration in the Italian Neogene succession (Pillans and Naish, 2004). At that time, the occurrence of “northern guest” molluscs in the Mediterranean fauna was considered as the first indication of significant climatic deterioration. Following these criteria, at the 19th International Geological Congress (Algiers, 1952), four Italian sections containing “northern guests” were considered as potential reference sections for the Pliocene/Pleistocene boundary: the Monte Mario section near Rome (Blanc et al., 1954), the Castell'Arquato section near Piacenza (Di Napoli, 1954), the Santerno section near Imola (Ruggieri, 1954), and

the Val Musone section near Ancona (Selli, 1954). None of these sections was subsequently accepted, but in 1977 the proposal for the location of the Pliocene/Pleistocene boundary stratotype at the Vrica section (Crotona, Calabria, southern Italy) was first proposed (Selli et al., 1977) and then formally ratified by IUGS in 1985 (Basset, 1985). Regardless, several authors consider the Monte Mario section, which contains the “northern guest” mollusc *Arctica islandica* at the base of the Pleistocene strata, a regional reference section of the Pliocene/Pleistocene boundary in central Italy.

The present multidisciplinary study on the Monte Mario succession was designed to allow us to compare it with the Vrica section and with other Mediterranean Pliocene/Pleistocene successions. Moreover, it provides indications about tectonic versus glacio-eustatic forcing in the evolution of the Pliocene–Pleistocene syn-rift sedimentary basins at the Tyrrhenian margin of the Apennines.

The marine sedimentary succession that crops out at Monte Mario and Monti della Farnesina (Rome, Italy, Fig. 1) has been studied since the early 19th century (Brocchi, 1820; Ponzi, 1872). Within the Monte Mario succession, these authors recognized the presence of a well-developed unconformity separating the Pleistocene strata from the underlying Pliocene sediments. Moreover, the Pliocene deposits were

* Corresponding author. Fax: +39 0654888201.

E-mail address: cosentin@uniroma3.it (D. Cosentino).

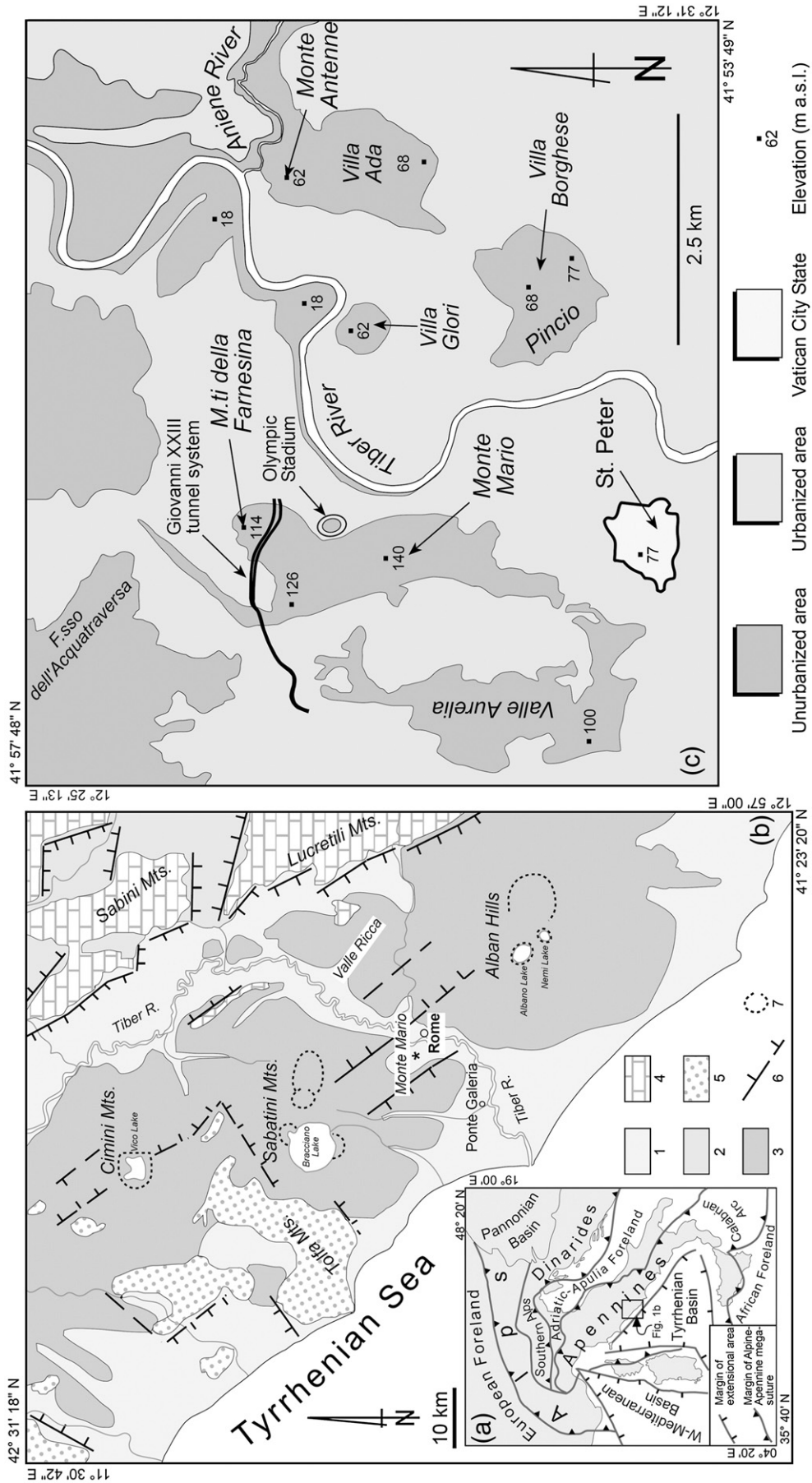


Figure 1. a) Structural sketch map of Italy and surrounding region. b) Geological sketch map of the central Italy Tyrrhenian margin. 1) Marine and continental deposits (Pliocene–Quaternary); 2) continental deposits (Villafranchian); 3) volcanics (Quaternary); 4) Meso-Cenozoic shallow- and deeper-water carbonates; 5) crystalline Paleozoic basement and sub-Ligurian (Cretaceous–Paleogene) allochthonous units; 6) extensional fault; 7) caldera and crater rim. c) Detail of the city map of Rome with the location of the Giovanni XXIII tunnel system.

cut by normal faults that did not affect the lower Pleistocene Monte Mario succession. During the 20th century, the authors who studied the Monte Mario succession accepted the stratigraphic and structural interpretations proposed in 1872 by Ponzi (Blanc, 1942; Blanc et al., 1953; Ambrosetti and Bonadonna, 1967; Bonadonna, 1968; Conato et al., 1980; Marra, 1993; Marra et al., 1995). The unconformity separating the Pliocene and Pleistocene deposits has been considered to be one of the most important features in the Neogene stratigraphy of central Italy. The regional importance of this unconformity allowed Blanc (1955) to define the “*Acquatraversa*” erosional phase, which is related to Late Pliocene climate change, as being responsible for the erosion of part of the Pliocene deposits (“*Marne Vaticane*” Auct.).

Recently, Carboni et al. (1993) and Bergamin et al. (2000) suggested that no unconformity separates the Pliocene strata from Quaternary deposits either at *Valle Ricca* (several km NE of Rome) (Carboni et al., 1993) or at Monte Mario (Bergamin et al., 2000). According to Bergamin et al. (2000), the boundary between the Pliocene and Pleistocene deposits in the Monte Mario succession is contained within a continuous regressive succession.

The aim of this paper is to better constrain stratigraphically the entire Monte Mario succession and to reinvestigate the Plio-Pleistocene boundary through new stratigraphical, structural, paleomagnetic, micropaleontological and palaeoecological data. New samples from the Plio-Pleistocene Monte Mario succession were obtained during the construction of the 2.5-km-long *Giovanni XXIII* tunnel through the Monti della Farnesina (Fig. 1c). Through these studies, we test the interpretation of Bergamin et al. (2000) that no unconformity exists at this important locality.

Geological setting

Since the late Serravallian (~12 Ma), Neogene extensional tectonics have controlled both the genesis and the evolution of sedimentary basins (i.e., syn-rift basins of the Tyrrhenian area; Mattei et al., 2002) in the hinterland of the Apennine–Maghrebian fold-and-thrust belt. These tectonic forces caused an extension of the previously thickened continental crust (Alpine–Apennine orogeny). Later extensional processes, occurring on higher angle normal faults in the period between the late Messinian (~6 Ma) to the early Pleistocene (Sartori, 1990; Sartori et al., 2004), contributed to the evolution of the present size and shape of the Tyrrhenian Basin. Besides controlling the evolution of the sedimentary basins, this later extensional stage triggered the Plio-Pleistocene volcanic activity that affected the peri-Tyrrhenian area (Locardi et al., 1977; Serri et al., 1993; Barberi et al., 1994; Cavinato et al., 1994; Montone et al., 1995; De Rita et al., 1995; Marra et al., 1998).

Rome is located on a downthrown block of the central Apennine fold-and-thrust belt (Fig. 1b), which was caused by post-orogenic extension that began in the late Messinian (~5.5 Ma) (Barberi et al., 1994; Cipollari et al., 1999; Cosentino et al., 2006). During the Plio-Pleistocene, relative sea-level changes linked to subsidence, uplift, and magmatic/volcanic processes induced transgressive/regressive cycles in the Rome area, northern Latium, and Tuscany (Barberi et al., 1994). Three Plio-Pleistocene sedimentary cycles have occurred in Tuscany and Latium (Barberi et al., 1994). The first cycle (A, Early Pliocene), consisting of blue-grey marls and clayey marls, extends from the *Sphaeroidinellopsis seminulina* s.l. Zone up to the *G. punctulata* Zone (5.33–3.22 Ma). It is truncated by the transgressive deposits of the second Pliocene cycle (B), which consists mainly of sands and biocalcarenes of the *G. aemiliana* Zone (Middle-Late Pliocene, 3.20–2.12 Ma) (Barberi et al., 1994). The third cycle (C) is included in the lower part of the early Pleistocene (~1.70–1.49 Ma) and consists of clayey sand deposits (Bonadonna, 1968; Ambrosetti et al., 1978, 1987; Barberi et al., 1994).

In exposures at Rome, deposits of Cycle C (Monte Mario Formation; Conato et al., 1980) lie directly on top of deposits of Cycle A (“*Marne*

Vaticane” Auct.). After deposition of the Monte Mario Formation, the middle Pleistocene sedimentary basins showed a complex regressive trend in the Rome area, shifting the Tyrrhenian coastline from Rome in the seaward direction to its present position (Ambrosetti and Bonadonna, 1967; Malatesta, 1978; Conato et al., 1980; Milli, 1997; Florindo et al., 2007).

Materials and methods

Mesostructural analyses

Mesostructural analyses were performed on 20 working faces during the advancement of the tunnel excavation, distributed between the Monte Vaticano and the Monte Mario formations. The direct measurement of fault planes and kinematic elements was limited to some extent by safety procedures related to unstable excavation fronts. Faults, joints, and kinematic data were processed using automated methods in the software DAISY3 (Salvini, 2004).

Paleontological analyses

For the paleontological analyses, 58 samples were examined from the Monte Vaticano and Monte Mario formations (Fig. 2). For the calcareous nannofossil studies, smear slides were prepared from the unprocessed samples using standard techniques and were analyzed with a light microscope at a magnification of 1000×. A quantitative analysis was carried out on selected calcareous nannofossils, except for the rare genus *Sphenolithus*. One hundred specimens of *Gephyrocapsa* were counted, following an informal classification of morphometric criteria: small *Gephyrocapsa* (<3.5 μm), medium *Gephyrocapsa* (larger than 3.5 μm and smaller than 5.5 μm), and large *Gephyrocapsa* (>5.5 μm). Furthermore, 100 specimens of *Pseudoemiliania lacunosa* (>4 μm) and *Reticulofenestra* spp., were counted as a unique group. The genus *Helicosphaera* was not abundant and only 10 to 30 specimens were counted. In the Pliocene samples, the abundance of the *Discoaster* group was also estimated. Unfortunately, the presence of this genus is discontinuous and shows strong variations in abundance. Nevertheless, where possible, discoasterids were also counted. Moreover, the abundances of *Sphenolithus* and *Calcidiscus* were estimated by counting the number of specimens per unit area (approximately 30 mm²).

For the ostracod and foraminifer analyses, each sample was disaggregated in a 5% H₂O₂ solution, washed through 0.063 and 0.125 mm coupled mesh sieves, and dried. For the ostracod analyses, where possible, approximately 300 valves were handpicked under the stereomicroscope and identified using SEM photos. The paleoenvironmental interpretation is based on the results of multivariate analyses illustrated in detail by Faranda et al. (2007).

The foraminifer biostratigraphy is based on the biozonal schemes of Cita (1975), Iaccarino (1985), Sprovieri (1992, 1993), and Iaccarino et al. (2007). The palaeoenvironmental interpretation of the foraminifer assemblages is based on autoecological and synecological data reported in Jorissen (1988), Murray (1991), Sgarrella and Moncharmont-Zei (1993), and Fiorini and Vaiani (2001).

Subdivisions of the marine neritic and oceanic benthic domain follow the classification schemes of Pérès (1982) and of Sgarrella and Moncharmont-Zei (1993): the infralittoral stage, which extends from the low tide level to a depth of 40–50 m and corresponds to the euphotic zone, and which is further subdivided into the upper infralittoral (from low-tide level to 25 m) and lower infralittoral (from 25 to 40–50 m); the circalittoral stage, which extends from 40–50 m to 150–200 m and corresponds to the oligophotic zone, and which is further subdivided into the upper circalittoral (from 40–50 to 80–100 m) and lower circalittoral (from 80–100 to 150–200 m); and the epibathyal stage, which extends from 150–200 m to 1000 m, and which is further subdivided into the upper epibathyal (from 150–200 to 400–500 m) and lower epibathyal (from 400–500 to 1000 m).

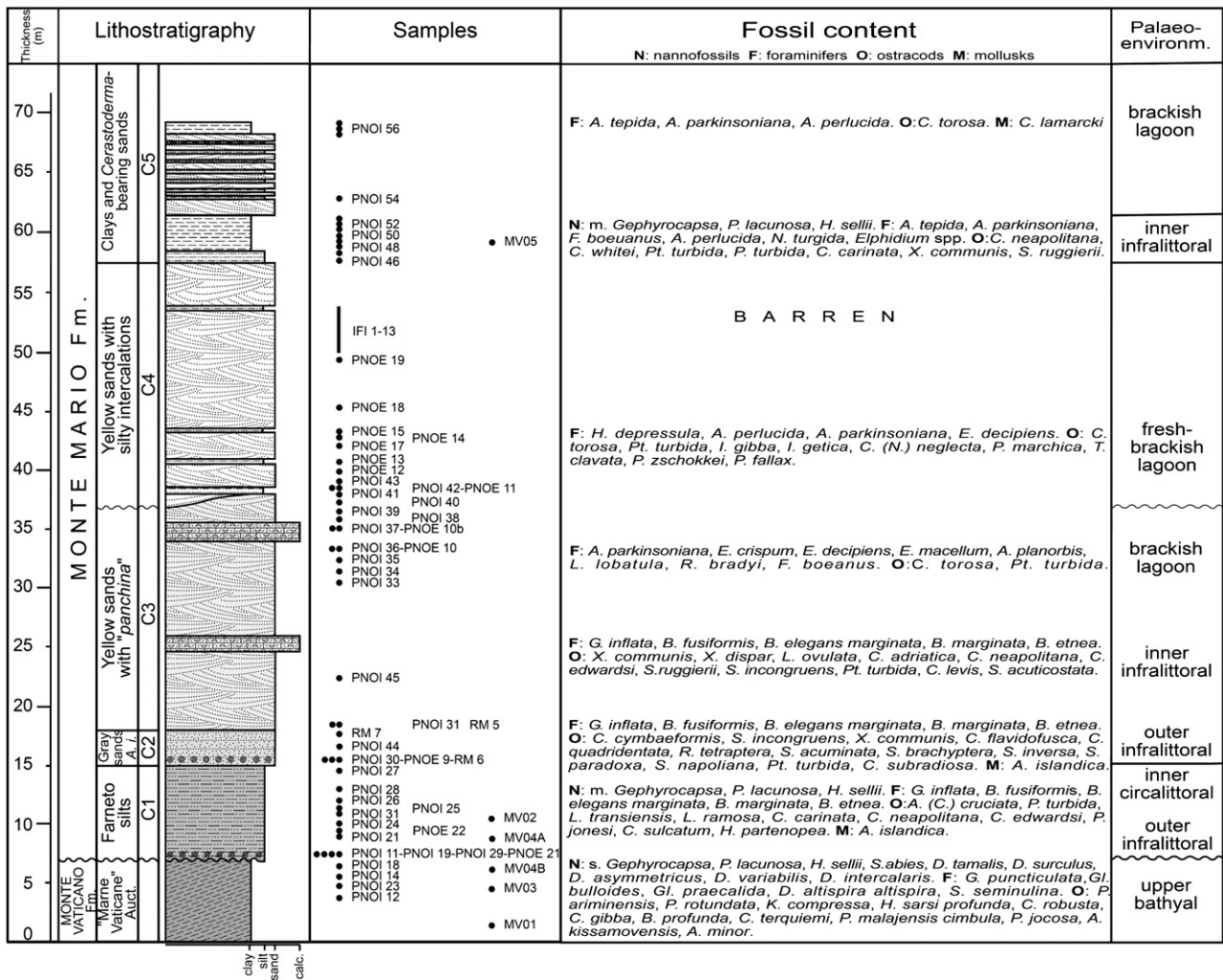


Figure 2. Stratigraphic column of the Monte Mario Plio-Pleistocene succession. Lithostratigraphy, collected samples, chronostratigraphy, fossil content, and palaeoenvironmental interpretation are shown. The PNOI, PNOE, RM and IFI samples are for palaeontological and sedimentological analyses, MV samples are for paleomagnetic investigations. Symbols at the base of the C1 and C2 members represent *A. islandica* levels.

Paleomagnetic analyses

Seventy-nine oriented cores from six sites located in the Monte Vaticano Formation and in the lower Monte Mario Formation were sampled (MV samples in Fig. 2). At each site, the cores were drilled and oriented *in situ* with a magnetic compass. The mean natural remnant magnetization (NRM) values ranged between 1.1×10^{-4} and 3.2×10^{-2} A/m. Samples from site MV05 were too weakly magnetized and showed unstable behavior during demagnetization, providing no reliable results. Samples were demagnetized using small field or temperature increments (5–10 mT or 30–50°C) up to the limit of reproducible results (60–80 mT or 400–520°C). Demagnetization diagrams were analyzed by principal component

analysis (Kirschvink, 1980) in order to determine the directions of characteristic remnant magnetization (ChRM) for each sample. Reliable results were obtained at five sites (Table 1). At three sites (MV01, MV02, and MV04A) the α_{95} was $<13^\circ$, whereas α_{95} was $>25^\circ$ at sites MV03 and MV04B. The high site-mean dispersions in the latter two sites are mostly related to the uneven magnetic properties of the Monte Vaticano Formation near the unconformity.

The Monte Mario succession: field and analytical data

The *Giovanni XXIII* tunnel system (Fig. 1c) was excavated through the historical site of the Monte Mario succession, tunnelling through

Table 1
Paleomagnetic directions and statistical parameters.

Sites (Formation, Member)	N (n)	Geographic coordinates				Stratigraphic coordinates		
		D	I	k	α_{95}	D	I	S ₀
MV01 (Monte Vaticano Fm)	12 (19)	171.4	−40.5	12.1	13	174.7	−31.6	290, 10
MV03 (Monte Vaticano Fm)	6 (10)	166.9	−55.6	8.3	25	156.8	−37.8	224, 20
MV04B (Monte Vaticano Fm)	4 (18)	195.5	−33.3	13.7	29	185.3	−39.1	168, 15
MV04A (Farneto silts Mb)	7 (11)	203.1	−66.4	43.1	9.4	197.0	−61.2	260, 6
MV02 (Farneto silts Mb)	8 (10)	198.9	−60.8	20.2	12.6	194.6	−55.4	260, 6

Note. N = number of demagnetised samples (n = number of sampled cores); D = declination (in degrees); I = inclination (in degrees); k = best estimate of the precision parameter; α_{95} = angular radius of the cone in which the mean direction lies within 95% confidence; S₀ = bedding attitude.

both the Monte Mario Formation (Cycle C) and the underlying Monte Vaticano Formation (“*Marne Vaticane*” Auct., Pliocene, Cycle A) (Fig. 2).

The Monte Vaticano formation (Cycle A)

The Monte Vaticano Formation consists of blue-grey marls and clayey marls punctuated by grey sands with a thickness of 10–20 cm. Observations made during the excavation confirmed the presence of a dense network of faults and fractures that cut the Monte Vaticano Formation and are truncated by the unconformity surface at the base of the Monte Mario Formation (Fig. 3).

The mesostructural data collected in Cycle A revealed a system of conjugate normal faults striking between NW–SE and NNW–SSE, and mostly dipping to the SW (Fig. 3c). Moreover, two subordinate systems, striking NE–SW and N–S and antecedent to the NW–SE system, were observed (Fig. 3d).

The fault planes are well-defined and show striae with dip-slip extensional kinematics. Both low- and high-angle normal faults were observed in the field. Low-angle faults generally show high cut-off angles, whereas high-angle faults generally show low cut-off angles (Fig. 3d). This observation suggests that tilting occurred during the extensional deformation.

The Monte Vaticano Formation is rich in microfossils. The nannoflora consist of common small *Gephyrocapsa* (100–150 specimens per mm²), *P. lacunosa* percentages higher than 10%, and *Helicosphaera sellii*, which represents more than 50% of the total

helicosphaerids (PNOI 23, PNOI 18). *Sphenolithus abies* specimens are always rare (<1 per mm²). The *Discoaster* group is represented by *D. tamalis* (25–40%), *D. surculus* (about 5% of discoasters), *D. asymmetricus* (<25%), and *D. variabilis* and *D. intercalaris* (not always present and never >10%). Foraminifers are also abundant and well-preserved, particularly in samples PNOI 14 and PNOI 23. Planktonic taxa are dominant and the benthonic fraction is well diversified. The marker *Globorotalia puncticulata* is always present and abundant. Sample PNOI 14 is characterized by a high frequency of *Dentoglobigerina altispira altispira*, which is known to characterize the uppermost Zanclean (~3.8–3.6 Ma) in the Latium coastal sites (Carboni and Di Bella, 1997). Ostracod assemblages are rather rich but are poorly diversified (only 25 species) (Fig. 2).

Paleomagnetic analyses showed a significant number of samples from the Monte Vaticano Formation with unstable behavior during both alternating field and thermal demagnetization. This behavior was observed mainly in samples from sites MV03 and MV04B and is probably related to their proximity to the angular unconformity, where some weathered sandy layers have been recognized. In most of the other samples, after the removal of a viscous component, a single component of magnetization was isolated in the intervals of 120–520°C (Figs. 4a, b) and 10–70 mT (Fig. 4c), suggesting titanomagnetite as the main magnetic carrier of NRM (Butler, 1992). Paleomagnetic results show that all the sites have a reversed polarity. The site-mean direction from the three sites in the Monte Vaticano Formation passes the Fold Test (McFadden, 1990) at the 95% confidence limit. Before

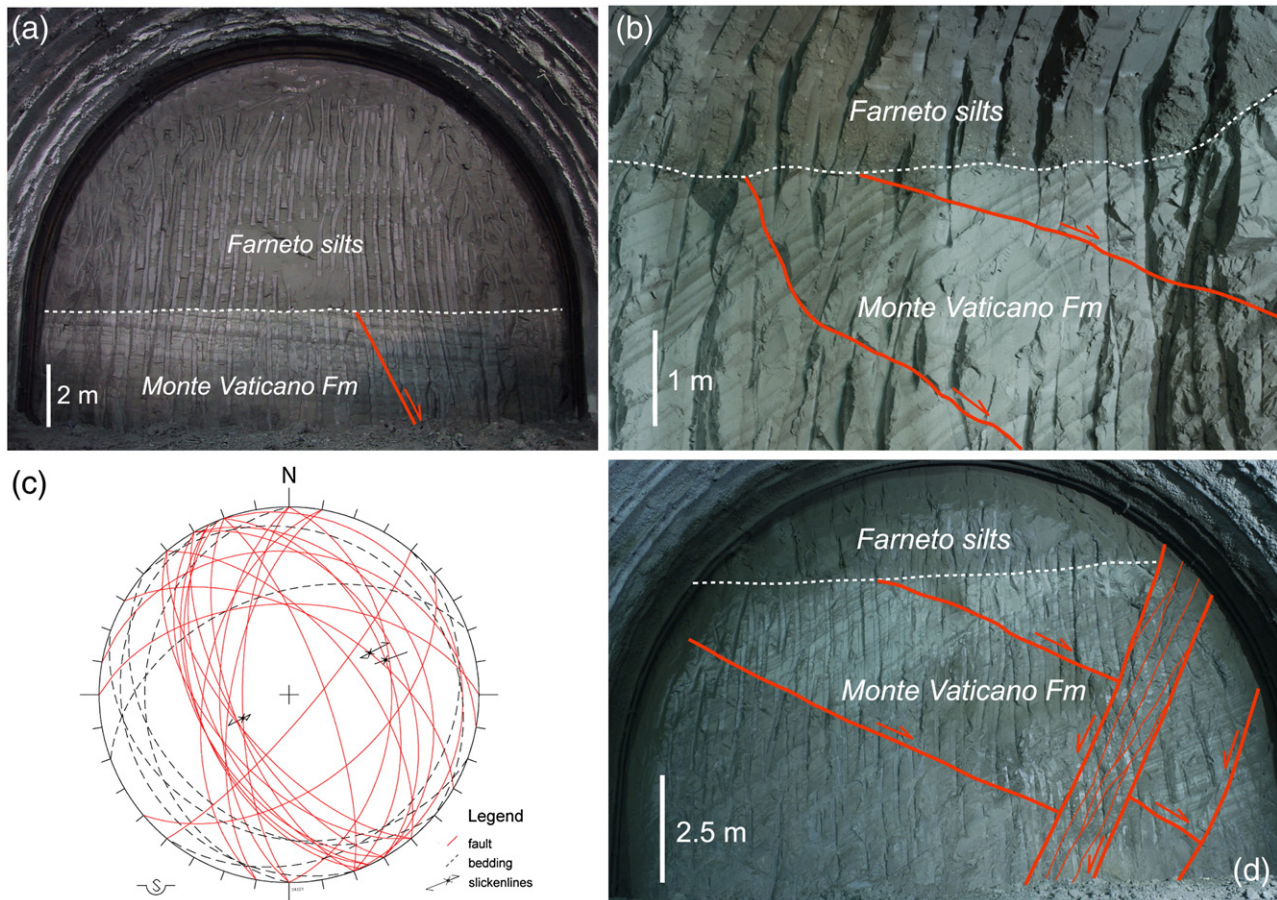


Figure 3. a) Unconformity surface between the Monte Vaticano Formation and the Monte Mario Formation (*Farneto silts*). An extensional fault plane affecting the Monte Vaticano marls is truncated by the overlying *Farneto silts* (*Giovanni XXIII* outer natural tunnel, at a distance of 950 m). b) Close up of the angular unconformity at the base of the Monte Mario Formation. As in panel a, two extensional faults affecting the Monte Vaticano Formation are truncated by the *Farneto silts* (*Giovanni XXIII* inner natural tunnel, at a distance of 907 m). c) Stereo plot (Schmidt net lower hemisphere) of the fault and bedding planes measured in the Monte Mario succession tunnelled by the *Giovanni XXIII* natural tunnel system (total number $n = 34$). The main fault system is NW–SE oriented and shows extensional kinematic indicators. The N–S and NE–SW fault planes seem to be antecedent with respect to the main NW–SE system. d) Unconformity surface between the Monte Vaticano Formation and the Monte Mario Formation (*Farneto silts*). The extensional fault planes truncated by the *Farneto silts* are cut by a NW–SE fault system dislocating the *Farneto silts*/Monte Vaticano Formation boundary (*Giovanni XXIII* inner natural tunnel, at a distance of 858 m).

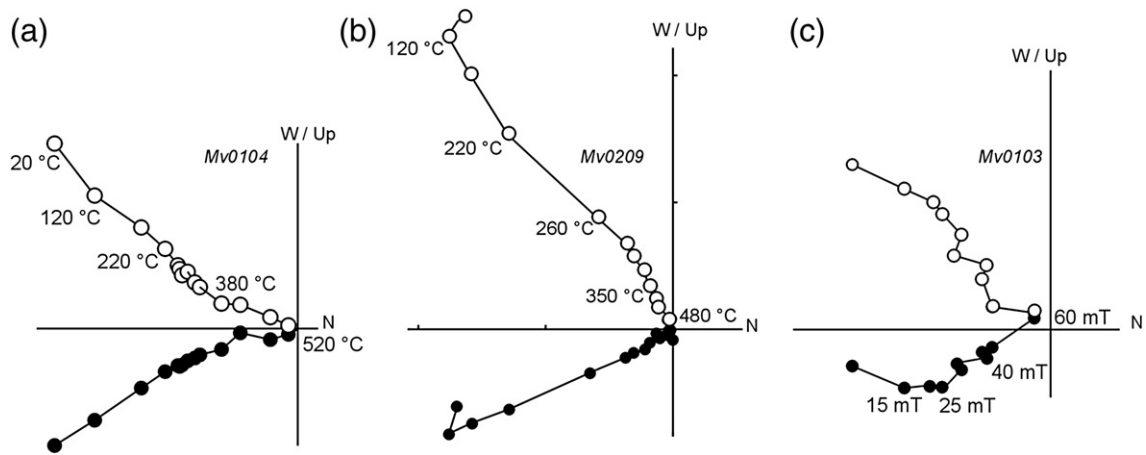


Figure 4. Vector component diagrams for the progressive thermal demagnetization of samples from Monte Vaticano Formation (a) and *Farneto silts* (b) and for alternating field demagnetization of a sample from Monte Vaticano Formation (c). Open and solid symbols represent projection on the vertical and horizontal planes, respectively.

tectonic correction, the mean ChRM vector is $D = 179.5^\circ$, $I = -43.8^\circ$, $\alpha_{95} = 24.9^\circ$, $k = 25.6$, whereas after tectonic correction the mean ChRM vector is $D = 172.3^\circ$, $I = -36.8^\circ$, $\alpha_{95} = 18.5^\circ$, $k = 45.0$ (Table 1).

The Monte Mario Formation (Cycle C)

Within the Monte Mario Formation, five members are distinguished (Fig. 2). From bottom to top, these members are:

- 1) *Farneto silts* (Member C1), corresponding to the “*Sabbie argillose grigie ad A. islandica*” p.p. of Bonadonna (1968) and to the “*Limi del Farneto*” of Marra (1993);
- 2) *Grey sands with A. islandica* (Member C2), corresponding to the “*Sabbie argillose grigie ad A. islandica*” p.p. of Bonadonna (1968) and to the “*Sabbie grigie ad A. islandica*” Auct.;
- 3) *Yellow sands with “panchina”* (Member C3), corresponding to the “*Sabbie gialle marine di Monte Mario*” of Bonadonna (1968);
- 4) *Yellow sands with silty intercalations* (Member C4);
- 5) *Clays and Cerastoderma-bearing sands* (Member C5).

Cycle C is affected mainly by high-angle normal faults striking NW–SE and NNW–SSE (Figs. 3c and d). The NW–SE trending Monte Mario horst, where this cycle crops out, is bounded on the NE by an extensional fault system (the *Acquatraversa* fault system), which was identified by Verri (1915). The *Giovanni XXIII* tunnel cuts through this important tectonic structure near the *Farnesina* entrance. The fault system is characterized by a 50-m-wide deformation zone oriented $N340^\circ 60'$, which juxtaposes the Monte Vaticano clays and the Monte Mario Formation in the hanging wall. At the *Farnesina* entrance, the hanging wall of the *Acquatraversa* fault system consists of Member C3 (*Yellow sands with “panchina”*) of the Monte Mario Formation, thus demonstrating approximately 35 m of throw of the base of the Monte Mario Formation. Another important extensional fault associated with the *Acquatraversa* fault system, which is oriented $N320^\circ 60'$, occurs inside the tunnel; at the surface, this fault can be traced NW along the *Fosso dell'Acquatraversa*.

Farneto silts (Member C1)

This member consists of approximately 8 m of sandy clays and clays. The lower boundary, which separates the underlying marls of Cycle A from the *Farneto silts*, was observed in both the inner and outer natural tunnels, and is an angular unconformity with erosive truncation of the Pliocene strata (Fig. 3). No internal bedding structures were observed in Member C1. The base is characterized by a 50-cm-thick horizon of fossiliferous clayey silt and glauconie grains occurring up to 2 m above the base. The basal shell layer marks the first occurrence of the “northern guest” *A. islandica* in

the stratigraphical record of the Monte Mario succession. The *Farneto silts* have a sharp upper boundary overlaid with *Grey sands with A. islandica*.

Calcareous nannofossil assemblages are characterized by the *Gephyrocapsa* group, which includes low percentages (~5%) of medium *Gephyrocapsa*; and the *Calcidiscus* group, which is composed entirely of *C. leptoporus*. Foraminifers are abundant and well-preserved. Samples include infralittoral assemblages with occasional epiphytal species such as *Quinqueloculina* spp., *Triloculina* spp., *Adelosina* spp., *Rosalina* spp., *Lobatula lobatula*, and *Asterigerinata* spp., circalittoral assemblages with increased frequency of *Buliminidae*, *Boliviniidae*, and *Cassidulinidae*, accompanied by typical circalittoral species such as *Valvulineria bradyana* and *Melonis pompilioides* and scarce planktonic taxa. Ostracods are abundant and are characterized by high-diversity assemblages (Fig. 2).

Paleomagnetic results show that all the sites sampled within Member C1 have reversed polarity. The site-mean direction from the two sites in the *Farneto silts* is $D = 200.8^\circ$, $I = -63.6^\circ$, $\alpha_{95} = 13.0^\circ$, $k = 379.7$ before tectonic correction, and $D = 195.7^\circ$, $I = -58.3^\circ$, $\alpha_{95} = 13.0^\circ$, $k = 379.7$ after tectonic correction (Table 1). Bedding in these sites dips gently NNW, with a homocline structure, which prevented us from performing a valuable fold test for the Member C1 sites. However, the mean inclination value from these sites is very high before tectonic correction ($I = 63.6^\circ$) and shallower afterwards ($I = 58.3^\circ$); the latter value is consistent with that expected at the Rome latitude after tectonic correction ($I = 60^\circ$).

Grey sands with A. islandica (Member C2)

Member C2 consists of a 3-m-thick fossiliferous coarse-medium grained grey sand. This is the previously described and well-known *A. islandica*-bearing horizon (Cerulli Irelli, 1905, 1908; Bonadonna, 1968; Ambrosetti and Bonadonna, 1967; Conato et al., 1980) rich in molluscs and including, in addition to *A. islandica*, two other “northern guests”: *Cochloidesma praetenuae* and *Buccinum humphreysianum* (Malatesta and Zarlenga, 1986). As for Member C1, no internal bedding structures were observed in Member C2, most likely as a result of bioturbation processes. This member undergoes a gradual transition into the overlying *Yellow sands with “panchina”* (Member C3).

Benthic foraminifers are abundant and well-preserved, and record an infralittoral environment. Planktonic foraminifers are scarce and represented by small-sized *Globorotalia inflata*, *Globorotalia oscitans*, *Globigerina* spp., and *Orbulina universa*. Ostracod assemblages from Member C2 are mainly characterized by phytal species, which represent 42% of the whole assemblage (Fig. 2). Among the collected ostracods, four “northern guest” species (*Bythocythere zetlandica*, *Cytheropteron depressum*, *Paradoxostoma*

ensiforme, and *Paradoxostoma abbreviatum*) were collected (Faranda et al., 2007; Faranda and Gliozzi, 2008).

Yellow sands with “panchina” (Member C3)

Member C3 consists of 18 m of medium to fine yellow sands with rare gravel intercalations. Thin, cemented sand layers and two biogenic carbonate horizons (“panchina”) rich in decalcified marine mollusc shells are also present. The internal bedding of Member C3 is characterized by large-scale trough cross-stratification, which represents sand-dune migration along a shoreline (upper shoreface). The boundary between Member C3 and the overlying *Yellow sands with silty intercalations* (Member C4) is present in the outer natural tunnel. It is characterized by an erosion surface that cuts into the *Yellow sands with “panchina”* as deeply as the second “panchina” horizon, dividing the Monte Mario Formation into two depositional sequences (MM1 and MM2) (Fig. 7).

Foraminifers and ostracods of Member C3 can be divided into two different groups: (1) those collected in the lower portion (samples PNOI 31, RM 5, and PNOI 45), which are similar to those recognized within Member C2; and (2) those collected in the upper portion (samples PNOI 33–40), which are characterized by rare and poorly preserved specimens of *Ammonia parkinsoniana*, *Florilus boeanus*, *Lobatula lobatula*, *Elphidium* spp., *Cyprideis torosa*, and *Pontocythere turbida* (Fig. 2).

Yellow sands with silty intercalations (Member C4)

The 22-m-thick Member C4 comprises beds, 3–10 m thick, of medium coarse-grained yellow sand with large-scale cross-stratifications. Each sand layer shows a coarsening-upward trend and is separated from the overlying sand by a thin horizon of yellow-grey silty clays, with symmetrical ripples located at the top of the coarse-grained sand.

Paleontological analyses confirm the presence of scarce benthic foraminifers. Ostracod assemblages are dominated by *Cyprideis torosa*, *Pontocythere turbida*, and halotolerant continental forms (Fig. 2).

Clays and Cerastoderma-bearing sands (Member C5)

Member C5 is characterised by 12 m of clays, silty clays, silts, and sands, which are thinly bedded in their upper part and contain the intertidal and estuarine species *Cerastoderma lamarcki*. In the basal portion, where the fine-grained fraction prevails (clays and silty clays), the nannoflora is characterized by *medium Gephyrocapsa*, which accounts for up to 50% of the *Gephyrocapsa* group. Foraminifer and ostracod assemblages are diversified, and they include the ostracod “warm guest” *Mediocytherideis (Sylvestra) virgula* (Faranda and Gliozzi, 2008). In the upper part (samples PNOI 52–PNOI 57), oligotypic assemblages are present, including *Cyprideis torosa*, *Ammonia parkinsoniana*, *Ammonia tepida*, and *Aubygnina perlucida* (Fig. 2).

Discussion

Chronostratigraphy

The paleontological analysis allows us to tightly constrain the age of both the Monte Vaticano (Cycle A) and the Monte Mario (Cycle C) formations (Fig. 5). The nannoflora of the Monte Vaticano Formation indicate an age younger than the last occurrence (LO) of *Reticulofenestra pseudoumbilicus*, which was never observed in the samples, and below the LO of *D. tamalis*, within the MNN16a Zone (Rio et al., 1990). Moreover, since *D. pentaradiatus* was also absent, the interval including the Monte Vaticano Formation probably falls within the paracme interval of *D. pentaradiatus* (Fig. 6). Finally, the presence of *S. abies*, although rare, together with the common occurrence of small *Gephyrocapsa*, which shows an acme interval just below the LO of *Sphenolithus* spp., suggests that the age of the Monte Vaticano Formation lies within the basal part of the MNN16a Zone (i.e., at the topmost part of the Zanclean, 3.84–3.70 Ma) (Cita et al. 1996). This age is confirmed by planktonic foraminifers corresponding to the *Globorotalia puncticulata* Zone (MPL 4a Subzone), which set the

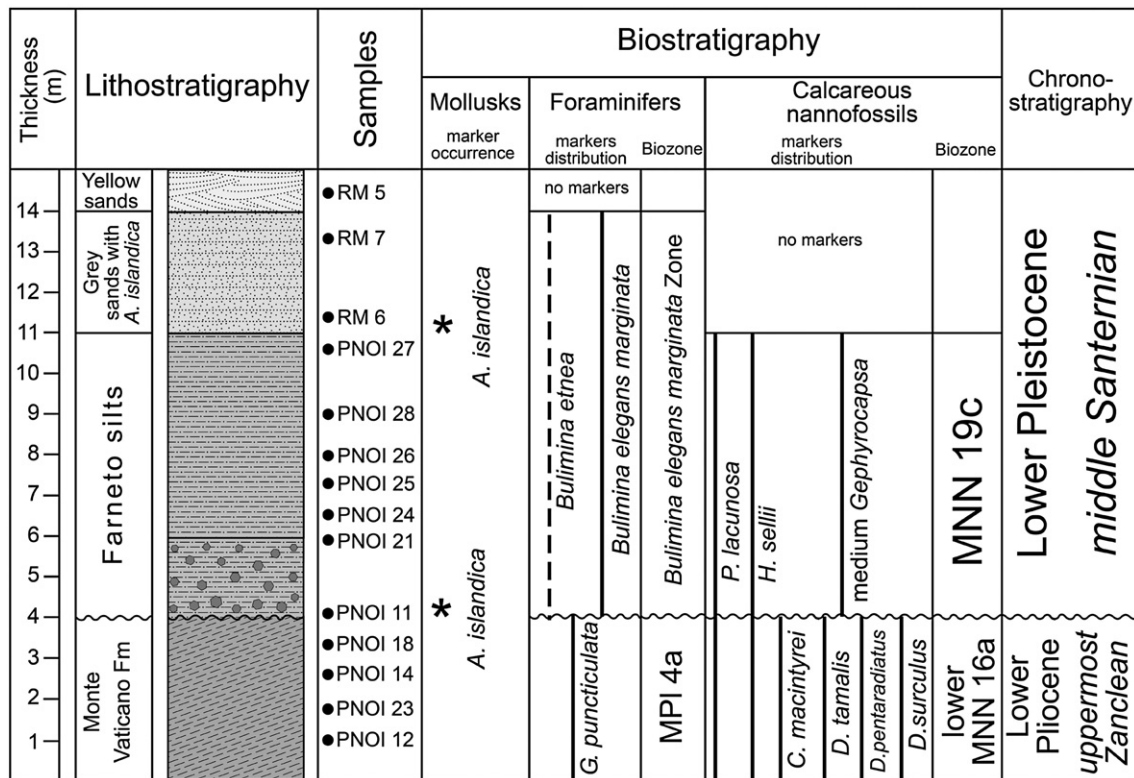


Figure 5. Litho-bio-chronostratigraphy across the unconformity surface between the Monte Vaticano and the Monte Mario formations. Dark circles in the basal part of the *Farneto* silts Member correspond to glauconic grains.

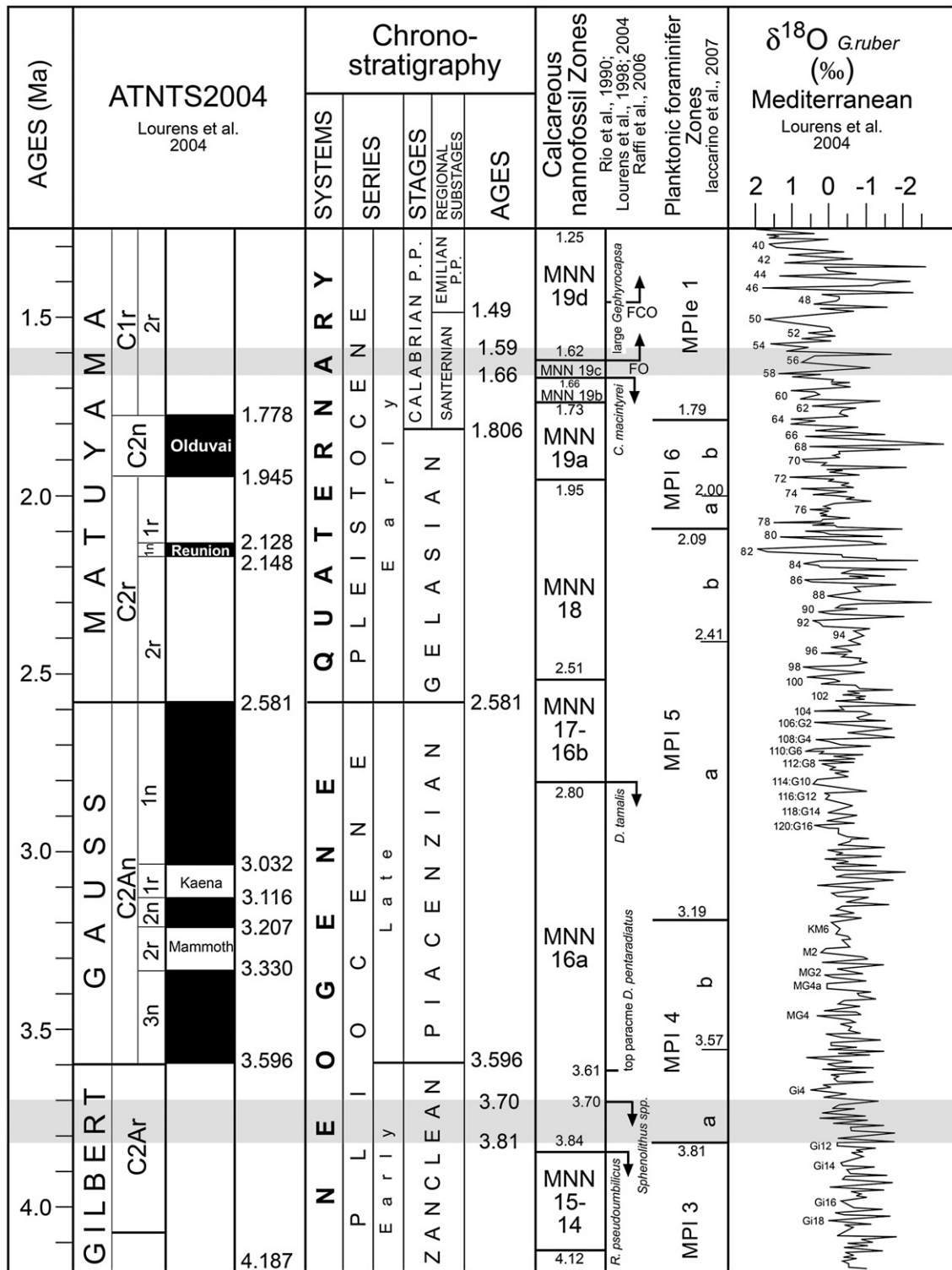


Figure 6. Pliocene-early Pleistocene magneto-bio-chronostratigraphical scheme, showing the position of the Monte Vaticano and Monte Mario formations. Oxygen isotope stratigraphy from Mediterranean benthic records (Lourens et al., 2004) is also shown. Calcareous nannofossil Zones are from Rio et al. (1990), Lourens et al. (1998; 2004), Raffi et al. (2006); planktonic foraminifer Zones are from Iaccarino et al. (2007).

boundaries for the time interval for the Monte Vaticano Formation at 3.81–3.70 Ma (Fig. 6).

According to the nannofossil data, the age of the whole Monte Mario Formation (Cycle C, Members C1–C5) is younger than both the first occurrence (FO) of medium *Gephyrocapsa* and the LO of *C. macintyrei*, and older than the FO of large *Gephyrocapsa* (MNN19c zone, Rio et al., 1990). In a recent revision of Pleistocene bio-horizons,

Raffi (2002) showed that the medium *Gephyrocapsa* spp. occurs for the first time in the Mediterranean area at 1.73 Ma. Since the top of *C. macintyrei* occurs at 1.66 Ma and the base of large *Gephyrocapsa* has been dated at 1.62 Ma (Lourens et al., 2004), the deposition of the Monte Mario Formation should span the interval between 1.66 Ma and 1.62 Ma. The occurrence of *Bulimina etnea* starting from the base of the Member C1 confirms an early Pleistocene age for the Monte Mario

Formation (middle Santernian, *Bulimina elegans marginata* Zone) (Fig. 5). It is worth noting that the FO of large *Gephyrocapsa* has been the subject of a recent controversy. Raffi et al. (1993) defined this biohorizon as slightly diachronous, occurring at 1.48 Ma [Marine Isotope Stage (MIS) 49/48 transition], whereas Wei (1993) considered it as consistently diachronous occurring between MIS 51 and MIS 47 at different sites. Applying high-resolution analyses at the Vrica section, Lourens et al. (1996) found the biohorizon at 1.59 Ma (during MIS 55). According to Raffi (2002), the large *Gephyrocapsa* are continuously and consistently present beginning three isotope stages above their first appearance, increasing in abundance in correspondence with MIS 51 and MIS 47.

Combining the age model from nannofossil biochronology with the occurrences of both northern and warm guests, the Monte Mario Formation can be tentatively correlated with the oxygen isotope stratigraphy from benthic records (Shackleton et al., 1990; Bassinot et al., 1994; Lourens et al., 2004). In particular, taking into account the occurrence of the top of *C. macintyre* at the MIS 59/58 transition in the Eastern Mediterranean (ODP Site 967), we can correlate the base of the Monte Mario Formation (Member C1 and Member C2), which bears *A. islandica* and other “northern guests”, with the MIS 58 glacial stage. Using the same approach, we can correlate the younger yellow sands with rich fossiliferous levels (Member C3) with the MIS 57 interglacial stage. Due to the poor reliability of the FO of large *Gephyrocapsa*, and taking into account the occurrence of warm guests at the top of the Monte Mario succession, we believe that Member C5 correlates with the MIS 55 interglacial stage (Fig. 7).

In this oxygen isotope stratigraphic framework, the sea-level drop responsible for the erosional surface separating the C3 and C4 members (MM1/MM2 boundary) is likely to correlate with the MIS 56 glacial

stage (Fig. 7). This indicates that MM1 and MM2 can be obliquity-forced (41 ka cycle) stratigraphic sequences within the early Pleistocene in the Rome area. The obliquity forcing in the early Pleistocene depositional sequences of the Monte Mario succession, as proposed in this paper, is in agreement with the general climatic signature of the early Pleistocene. According to the oxygen isotope stratigraphy, obliquity had a significant role in forcing the stratigraphic signal during the entire Matuyama chron (2.58–0.7 Ma), whereas the eccentricity (100-ka cycle) was dominant during the last 650 ka of the Pleistocene (Ruddiman et al., 1986; Shackleton, 1995; Williams et al., 1998).

The chronostratigraphical indications obtained from the paleontological analyses are in full agreement with the paleomagnetic data, which indicate a reversed polarity for samples from both Cycle A and Cycle C. As a consequence, the reverse polarity of the Monte Vaticano Formation (Cycle A) can be correlated with the uppermost Gilbert reversed epoch (C2Ar), and the reversed polarity of the *Farneto silts* (member C1) with the middle Matuyama reversed epoch (C1r2r) (Fig. 6).

Palaeoenvironments and sequence stratigraphic interpretation

The analyses of the foraminifer and ostracod assemblages collected from the deposits of the Monte Vaticano and Monte Mario formations have increased our knowledge of the palaeoenvironmental and paleoecological evolution of the succession. Paleocological data obtained from the multivariate analyses of ostracod assemblages (Faranda et al., 2007) and qualitative palaeoenvironmental data inferred from foraminifers are presented here in a sequence stratigraphy perspective.

The portion of the Monte Vaticano Formation (Cycle A) examined in this study corresponds to an upper epibathyal environment (Fig. 8),

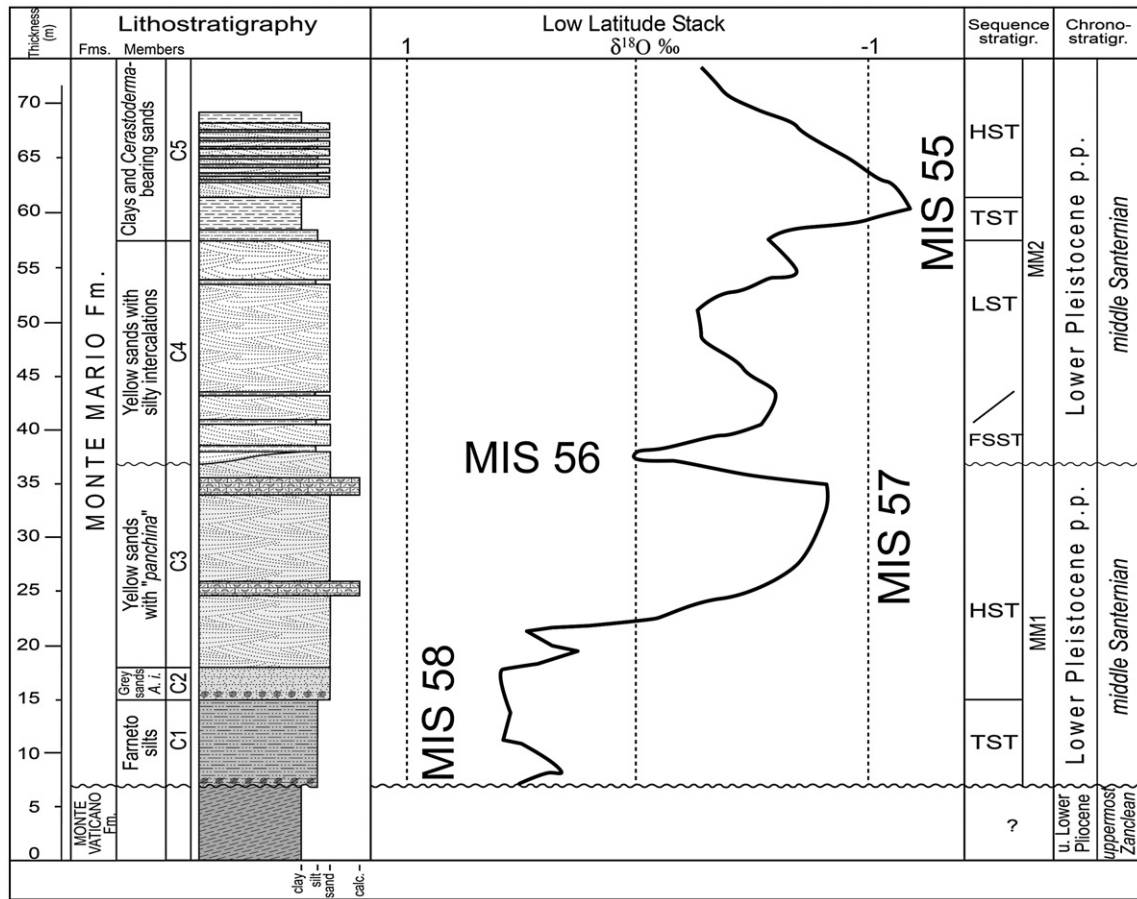


Figure 7. Litho- and chrono-sequence stratigraphy of the Monte Mario Formation vs. oxygen isotope stratigraphy from low-altitude stack of benthic records (Shackleton et al., 1990; Bassinot et al., 1994; Lourens et al., 2004). Legend: TST - transgressive systems tract; HST - highstand systems tract; FSST - falling stage systems tract; LST - lowstand systems tract. See text for explanations.

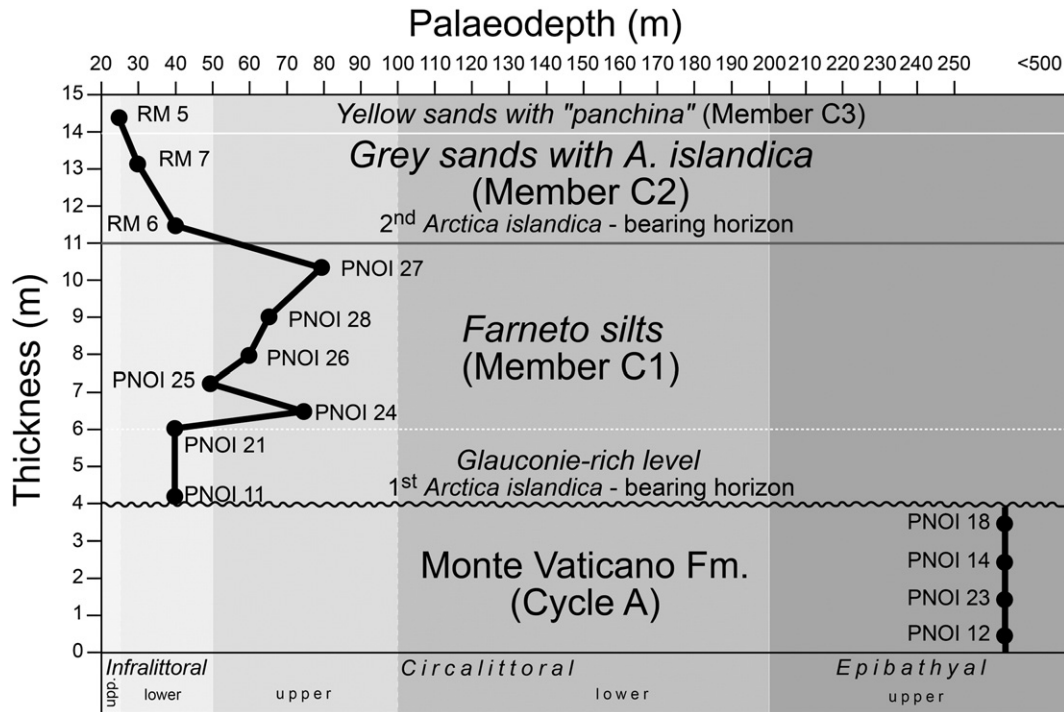


Figure 8. Relative sea-level changes in the lower portion of the Monte Mario Formation. See text for explanations.

probably with a depth of approximately 300–350 m, based on the high P/B (Plankton/Benthic) ratio, the autoecological signal from the benthic foraminiferal taxa and the presence, among ostracods, of deep-sea species such as *Henryhowella sarsii profunda*, *Kriethe compressa*, *Parakriethe ariminensis*, *Parakriethe rotundata*, *Bairdoppilata profunda*, *Cytherella terquemi*, *Cytherella robusta*, and *Cytherella gibba*. The extensional faults affecting the Monte Vaticano Formation (Cycle A), which are truncated by the overlying Farneto silts (Cycle C, Member C1), suggest the occurrence of a tectonic phase pre-dating the deposition of the Monte Mario Formation (Cycle C). Contrary to what was reported in Bergamin et al. (2000), there is a well-developed unconformity between the Monte Vaticano and the Monte Mario formations, which is characterized by erosional truncation of the Pliocene strata and which defines the lower sequence boundary (SB) of the Monte Mario third-order sequence. The Member C1 rests just above this SB and bears mollusc fragments and glauconie grains (Figs. 2 and 8), suggesting a ravinement surface that separates the Monte Vaticano and the Monte Mario formations.

Above the unconformity, the Monte Mario Formation (Cycle C) corresponds to a littoral environment (low P/B ratio among foraminifers), which has undergone several relative sea-level fluctuations. In fact, ostracods and foraminifers at the bottom (Member C1) testify to the existence of a lower infralittoral environment (approximately 40 m deep), which gradually evolves into a deeper upper circalittoral environment down to 70–75 m deep (sample PNOI 24). Upwards in the succession, the ostracod assemblages record the restoration of infralittoral conditions (approximately 50 m deep, sample PNOI 25) and progressive deepening down to 80 m (sample PNOI 27) (Fig. 8). These two relative sea-level changes are responsible for a retrogradational stacking pattern in an offshore setting, which defines a transgressive systems tract (TST) at the base of the Monte Mario Formation.

At the bottom of both the C1 and C2 members, "northern guests" occur among the fossil contingent (only *A. islandica* at the base of the C1 member and three mollusc and four ostracod species at the base of the C2 member), reflecting a remarkable water temperature decrease (Malatesta and Zarlenga, 1986; Faranda et al., 2007) that may correlate

to the MIS 58 glacial period. Several papers have noted the occurrence of cold indicator molluscs and ostracods, species whose normal geographic distribution is only outside the Mediterranean Sea at higher latitudes. Their presence in the Mediterranean area in sedimentary deposits recognized as early Pleistocene and Pleniglacial [see reviews in Malatesta and Zarlenga (1986) for molluscs, and in Ruggieri (1980) for ostracods], is consistent with regional cooling at these times.

The foraminifers and, particularly, the ostracods of Member C2 and Member C3 testify to three shallowing-upward episodes. The first is from a lower infralittoral environment (40–30 m, samples RM 6–7) to an upper infralittoral, vegetated environment (approximately 25 m, samples RM 5, PNOI 45). The second is from a lower infralittoral environment (30 m, PNOI 33) to a brackish lagoonal environment (less than 10 m, PNOI 34–PNOI 36), and the third is from a lower infralittoral environment (35 m, PNOI 37) to a brackish lagoonal environment (less than 10 m, PNOI 38–40) (Faranda et al., 2007). During the last two oscillations, it is likely that the shallow environments were established and a salinity drop occurred, as indicated by the presence of scarce *Cyprideis torosa*, a very shallow-water dweller and a strongly eurihaline species (Lachenal, 1989; Neale, 1988; Meisch, 2000, and refs. therein). In terms of sequence stratigraphy, these shallowing-upward episodes recognized in the Monte Mario sands may be interpreted as parasequences (fifth- or higher-order changes in sea-level) within a highstand systems tract (HST) developed in upper shoreface-backshore environments.

In Member C4, which rests unconformably above Member C3, scarce ostracod and foraminifer assemblages are recorded, testifying to a very shallow (<10 m) and brackish environment in a backshore setting. The silty intercalations that characterize this member (PNOI 41–42 and PNOE 13) record several oligohaline episodes, as indicated by the presence of freshwater/oligohaline species, with halotolerant continental forms (upper coastal plain). Going upwards from this zone (PNOE 18–IFI 13), the samples are barren. Thus, the backshore/upper coastal plain environments recorded in Member C4, in contrast with the upper shoreface of the underlying Member C3, should represent a falling stage/lowstand systems tract deposited just after

the relative sea-level drop responsible for the erosional surface (SB) that separates Members C3 and C4 of the Monte Mario Formation (Fig. 2). This sea-level drop may correlate to the MIS 56 glacial period.

The ostracod and foraminifer assemblages from the basal portion of Member C5 indicate the restoration of upper infralittoral (~15–20 m deep) marine conditions (samples PNOI 46–51), recording a second marine transgression (TST) within the Monte Mario Formation. Within the upper portion of this member, a short interval (PNOI 52–55) shows scarce and poorly preserved ostracods, represented primarily by juveniles of *Cyprideis*, *Pontocythere*, and *Candoninae*. At the top of the succession, two samples (PNOI 56–57) bear monospecific *Cyprideis torosa* assemblages and abundant *Ammonia* spp. and *C. lamarcki*. Most likely, they indicate a very shallow brackish marginal marine environment characterized by poorly oxygenated waters, showing a progradational stage for the uppermost portion of the Monte Mario Formation (HST).

Tectonics

Many authors have reported the presence of faults and fractures in the Monte Mario Pliocene–Pleistocene succession (Ponzi, 1875; Tellini, 1893; Verri, 1915). The structural data reported in this paper indicate that the Pliocene–lower Pleistocene deposits in the area of Rome were affected by two tectonic phases. Taking into account the Plio–Pleistocene regional stratigraphic framework of northern Latium and Tuscany (Barberi et al., 1994), the first tectonic phase may have occurred at the Pliocene/Pleistocene transition, affecting only the marine clays of the Monte Vaticano Formation (Cycle A) with NE–SW trending extensional faults. As a consequence of this tectonic phase, the area underwent uplift that, combined with the glacio-eustatic sea-level changes at MIS 58, resulted in a total relative sea-level drop of approximately 260 m, since lower infralittoral (40 m deep) deposits (Farneto silts, Member C1) rest unconformably above the upper epibathyal clays of Cycle A.

Is this sea-level drop, which is calculated at the Early Pliocene/early Pleistocene boundary of the Monte Mario succession, representative of what happened at the Late Pliocene/early Pleistocene transition? The occurrence of the Late Pliocene Tyrrhenian coastline at the foothill of the Lucretili Mountains (Cosentino and Fubelli, 2008), very close to the position of the Early Pliocene Tyrrhenian coastline (Monte Vaticano Formation) as recently reconstructed by Cosentino et al. (2008), allow us to consider the paleodepth of the Late Pliocene sediments in the Rome area quite similar to the paleodepth of the Monte Vaticano Formation. The Gelasian (Upper Pliocene, Cycle B) clays and silty clays recovered in boreholes drilled near the Tiber River in the city of Rome (Carboni and Iorio, 1997) indicate paleodepth similar to the Monte Vaticano Formation and strengthen this conclusion.

The second tectonic phase, which affects the Monte Mario Formation (Cycle C) with NW–SE high-angle normal faults, occurred in post-Santernian times and was responsible for the present morpho-structural setting of the Monte Mario–Gianicolo area in Rome. According to Funicello and Giordano (2008), the last tectonic uplift of the Monte Mario area occurred between 0.75 and 0.62 Ma, causing a southwest deviation of the paleo-Tiber River near Rome.

Concluding remarks

The analyses performed on the Monte Mario succession recently exposed by the *Giovanni XXIII* tunnel system provide much useful information about chronostratigraphy, sequence stratigraphy, paleoenvironmental evolution, and tectonics of the Plio–Pleistocene succession that crops out within the city of Rome.

The succession has been split into two formations: the Monte Vaticano Formation and the Monte Mario Formation, pertaining to regional sedimentary cycles A (Early Pliocene) and C (early Pleisto-

cene), respectively. Calcareous nannofossils, foraminifers, and paleomagnetic analyses place the time of deposition of the Monte Vaticano Formation at the top of the Zanclean (3.81–3.70 Ma) (uppermost Gilbert reversed epoch, C2Ar), and place the time of deposition of the Monte Mario Formation at the early Pleistocene (middle Santernian, 1.66–1.59 Ma) (middle Matuyama reversed epoch, C1r2r). According to Bergamin et al. (2000), no major unconformity characterizes the Pliocene/Pleistocene transition in the Monte Mario section. In contrast, our biostratigraphical data point to a stratigraphical gap of approximately 2 Ma between the Monte Vaticano and the Monte Mario formations, which are separated by a major angular unconformity, characterized by erosional truncation of the underlying Pliocene strata.

Comparing the biostratigraphy of the Monte Mario succession with those of Vrica and ODP Site 967 (Raffi, 2002) and taking into account their oxygen isotope stratigraphy, the Monte Mario Formation recorded two early Pleistocene glacial–interglacial oscillations, corresponding to MIS 58/57 and MIS 56/55. The lower Pleistocene (middle Santernian) transgression occurred on a highly tectonized Pliocene substratum, which was affected by both NE–SW and N–S striking extensional faults. This tectonic phase was responsible for regional uplift in central Italy, which induced erosional processes mainly on the Tyrrhenian side of the Apennines (*“Acquatraversa”* erosional phase, Bonadonna, 1968). Besides the tectonically induced sea-level changes, a glacio-eustatic contribution to the 260-m relative sea-level drop can be inferred from the presence of “northern guests” at the base of Monte Mario Formation (C1 and C2 members), implying cold climate conditions (MIS 58 glacial stage). The sudden disappearance of “northern guests” in the younger Monte Mario yellow sands (Member C3), which partly correspond to the same infralittoral environment, is most likely linked to more temperate conditions (MIS 57).

The unconformity within the Monte Mario Formation, which distinguishes two depositional sequences (MM1 and MM2), may be related to the sea-level drop induced by a younger glacial stage (MIS 56), followed by an interglacial period (MIS 55). This interpretation is supported by the occurrence of “warm guests” in the basal clays of the topmost Monte Mario member (Member C5).

The sedimentological and paleoenvironmental investigations allow us to suggest a possible sequence stratigraphy interpretation of the Monte Mario succession. In this interpretation, the unconformity between the Monte Vaticano and Monte Mario formations may define the lower SB of the Monte Mario third-order depositional sequence, which originated with a tectono-eustatic sea-level drop. Within the Monte Mario Formation, two depositional sequences (MM1 and MM2, Fig. 7) characterized by transgressive systems tracts of littoral marine environments have been recognized. Within MM1, the base of the *Farneto silts* corresponds to a transgressive surface, whereas the transition between *Farneto silts*/*Grey sands with A. islandica* can be interpreted as a maximum flooding surface separating the TST (*Farneto silts*) from the HST (*Grey sands with A. islandica* – *Yellow sands with “panchina”*). The erosional surface recognized at the base of the *Yellow sands with silty intercalations* represents the lower SB of the MM2 depositional sequence induced by a glacio-eustatic sea-level drop (MIS 56). The upper infralittoral clays at the base of the *Clays and Cerastoderma-bearing sands*, which contain “warm guests”, correspond to the TST of the MM2 depositional sequence, whereas the overlying coarse-grained deposits define its HST. Taking into account the age model suggested in this paper for the Monte Mario Formation, MM1 and MM2 may correspond to two glacio-eustatic sequences cyclically induced by changes in the obliquity of the Earth’s axis (the 41-ka cycle).

Acknowledgments

The authors are grateful to *Astaldi Spa* for the permission to follow the excavation of the *Giovanni XXIII* tunnel system and for the financial

support of this work. Thanks are also due to two anonymous referees whose suggestions definitely improved this paper. We are indebted to QR Editors D. Booth, J. Knox, and D. Muhs for their valuable comments and editing hints. Finally we are thankful to J. Knox and D. Muhs for the English revision.

References

- Ambrosetti, P., Bonadonna, F.P., 1967. Revisione dei dati sul Plio-Pleistocene di Roma. *Atti della Accademia Gioenia di Scienze Naturali in Catania* 18, 33–81.
- Ambrosetti, P., Carboni, M.G., Conti, M.A., Costantini, A., Esu, D., Gandin, A., Girotti, O., Lazzaretto, A., Mozzanti, R., Nicosia, U., Parisi, G., Sandrelli, F., 1978. Evoluzione paleogeografica e tettonica dei bacini toscano-umbro-laziali nel Pliocene e nel Pleistocene inferiore. *Memorie della Società Geologica Italiana* 19, 573–580.
- Ambrosetti, P., Carboni, M.G., Conti, M.A., Esu, D., Girotti, O., La Monica, G.B., Landini, B., Parisi, G., 1987. Il Pliocene ed il Pleistocene inferiore del Bacino del Fiume Tevere nell'Umbria meridionale. *Geografia Fisica e Dinamica Quaternaria* 10, 10–33.
- Barberi, F., Buonasorte, G., Cioni, R., Fiordelisi, A., Foresi, L., Iaccarino, S., Laurenzi, M.A., Sbrana, A., Vernia, L., Villa, I.M., 1994. Plio-Pleistocene geological evolution of the geothermal area of Tuscany and Latium. *Memorie Descrittive della Carta Geologica d'Italia* 49, 77–134.
- Basset, M.G., 1985. Towards a "common language in stratigraphy". *Episodes* 8, 87–92.
- Bassinot, F.C., Beaufort, L., Vincent, E., Labeyrie, L., Rostek, F., Müller, P.J., Quidelleur, X., Lancelot, Y., 1994. Coarse fraction fluctuations in pelagic carbonate sediments from the tropical Indian ocean: a 1500-kyr record of carbonate dissolution. *Paleoceanography* 9, 579–600.
- Bergamin, L., Carboni, M.G., Di Bella, L., Marra, F., Palagi, I., 2000. Stratigraphical and paleoenvironmental features of the Pleistocene sediments of M. Mario (Rome). *Eclogae Geologicae Helveticae* 93, 265–275.
- Blanc, A.C., 1942. Variazioni climatiche ed oscillazioni della linea di riva nel Mediterraneo centrale durante l'Era Glaciale. *Geologie d. Meere u. Binnengewässer* 5, 137–219.
- Blanc, A.C., 1955. Ricerche sul Quaternario Laziale. III – Avifauna artica, crioturbazioni e testimonianze di soliflussi nel Pleistocene medio-superiore di Roma e di Torre in Pietra. Il periodo glaciale Nomentano nel quadro della serie di glaciazioni riconosciute nel Lazio. *Quaternaria* 2, 187–200.
- Blanc, A.C., Tongiorgi, E., Trevisan, L., 1953. Le Pliocène et le Quaternaire aux alentours de Rome. *INQUA IV^e Congrès International – Roma Pisa, 1953. Programme des excursions aux alentours de Rome* 1–35.
- Blanc, A.C., Tongiorgi, E., Trevisan, L., 1954. La limite Plio-Pleistocène dans la coupe de Monte Mario (environs de Rome). *Congrès Géologique International, Comptes Rendus de XIX Session, Alger 1952* 15, 218–228.
- Bonadonna, F.P., 1968. Studi sul Pleistocene del Lazio. V – La biostratigrafia di Monte Mario e la "Fauna Malacologica Mariana" di Cerulli Irelli. *Memorie della Società Geologica Italiana* 7, 261–321.
- Brocchi, G., 1820. Dello stato fisico del suolo di Roma ed illustrazione della carta geognostica di questa città. *Stamperia di Romanis*, 281 pp., 1 carta geologica.
- Butler, R.F., 1992. *Paleomagnetism: Magnetic Domains to Geologic Terranes*. Blackwell Scientific Publications, Boston, MA, p. 319.
- Carboni, M.G., Di Bella, L., 1997. The Plio-Pleistocene of the Anzio coast (Rome). *Bollettino della Società Paleontologica Italiana* 36 (1–2), 135–159.
- Carboni, M.G., Iorio, D., 1997. Nuovi dati sul Plio-Pleistocene marino del sottosuolo di Roma. *Bollettino della Società Geologica Italiana* 116, 435–451.
- Carboni, M.G., Di Bella, L., Girotti, O., 1993. Nuovi dati sul Pleistocene di Valle Ricca (Monterotondo, Roma). *Il Quaternario* 6, 39–48.
- Cavinato, G.P., Cosentino, D., De Rita, D., Funicello, R., Parotto, M., 1994. Tectonic-sedimentary evolution of intrapenninic basins and correlation with the volcano-tectonic activity in Central Italy. *Memorie Descrittive della Carta Geologica d'Italia XLIX*, 63–76.
- Cerulli Irelli, S., 1905. Sopra i molluschi fossili del Monte Mario presso Roma. *Bollettino della Società Geologica Italiana* 24, 191–194.
- Cerulli Irelli, S., 1908. Fauna malacologica mariana. Parte seconda – *Leptonidae, Galeommatidae, Cardidae, Chamidae, Cyprinidae, Veneridae*. *Paleontografia Italiana* 14, 1–64.
- Cipollari, P., Cosentino, D., Gliozzi, E., 1999. Extension- and compression-related basins in central Italy during the Messinian *Lago-Mare* event. *Tectonophysics* 315, 163–185.
- Cita, M.B., 1975. Studi sul Pliocene e sugli strati di passaggio dal Miocene al Pliocene VIII. Planktonic foraminiferal biozonation of the Mediterranean Pliocene deep sea record. A revision. *Rivista Italiana di Paleontologia* 81, 527–544.
- Cita, M.B., Rio, D., Hilgen, F., Castradori, D., Lourens, L., Vergerio, P.P., 1996. Proposal of the Global Boundary Stratotype Section and Point of the Piacenzian stage (middle Pliocene). *Inter. Comm. On Stratigr. Subcomm. On Neogene Stratigraphy*.
- Conato, V., Esu, D., Malatesta, A., Zarlenga, F., 1980. New data on the Pleistocene of Rome. *Quaternaria* 22, 131–176.
- Cosentino, D., Fubelli, G., 2008. Comment on: "Geomorphological, paleontological and ⁸⁷Sr/⁸⁶Sr isotope analyses of early Pleistocene paleoshorelines to define the uplift of Central Apennines (Italy)". *Quaternary Research* 69, 163–164.
- Cosentino, D., Federici, I., Cipollari, P., Gliozzi, E., 2006. Environments and tectonic instability in central Italy (Garigliano Basin) during the late Messinian *Lago-Mare* episode: new data from the onshore Mondragone 1 well. *Sedimentary Geology* 188–189, 297–317.
- Cosentino, D., Castorina, F., Cipollari, P., Fubelli, G., 2008. Pliocene paleoshorelines and uplift rates at the Tyrrhenian margin of central Apennines (Italy). *GEOSD 2008, Bari 23–27 settembre 2008. Abstracts*: 39–41.
- De Rita, D., Faccenna, C., Funicello, R., Rosa, C., 1995. Stratigraphy and volcano-tectonics. In: Trigila, R., (Ed.), *The Volcano of the Alban Hills*. Università degli Studi di Roma "La Sapienza", Rome, 33–71.
- Di Napoli, E., 1954. La limite Plio-Pleistocène dans la coupe de Castell'Arquato (Plaisance). *Congrès Géologique International, Comptes Rendus de XIX Session, Alger 1952. Volume 15*: 229–234.
- Faranda, C., Gliozzi, E., 2008. The ostracod fauna of the Plio-Pleistocene Monte Mario succession (Roma, Italy). *Bollettino della Società Paleontologica Italiana*, 43(3), (in press), Modena.
- Faranda, C., Gliozzi, E., Mazzini, I., 2007. Palaeoenvironmental evolution of the Plio-Pleistocene Monte Mario succession (Rome, Italy) inferred from ostracod assemblages. *Rivista Italiana di Paleontologia e Stratigrafia* 113 (3), 473–485.
- Fiorini, F., Vaiani, S.C., 2001. Benthic foraminifer and transgressive-regressive cycles in the Late Quaternary subsurface sediments of the Po Plain near Ravenna (Northern Italy). *Bollettino della Società Paleontologica Italiana* 40 (3), 357–403.
- Florindo, F., Karner, D.B., Marra, F., Renne, P., Roberts, A., Weaver, R., 2007. Radiometric age constraints for glacial terminations IX and VII from aggradational sections of the Tiber River delta in Rome, Italy. *Earth and Planetary Science Letters* 256, 61–80.
- Funicello, R., Giordano, G., 2008. Note illustrative della Carta Geologica d'Italia alla scala 1:50.000, foglio 374 – Roma. APAT – Servizio Geologico d'Italia, pp. 158.
- Iaccarino, S., 1985. Mediterranean Miocene and Pliocene planktic foraminifera. In: Bolli, H.H., Sanders, J.B., Perck-Nielsen, K. (Eds.), *Plankton Stratigraphy*, pp. 283–314.
- Iaccarino, S.M., Premoli Silva, I., Biondi, M., Foresi, L.M., Lirer, F., Turco, E., Petrizzi, M.R., 2007. *Practical Manual of Neogene Planktonic Foraminifera*. International School on Planktonic Foraminifera, 6th course, Perugia 19–23 February 2007, University of Perugia, 1–181.
- Jorissen, F.J., 1988. Benthic foraminifera from the Adriatic Sea; principles of phenotypic variations. *Utrecht Micropaleontological Bulletin* 37, 1–174.
- Kirschvink, J.L., 1980. The least-square line and plane and the analysis of paleomagnetic data. *Geophysical Journal of Royal Astronomical Society* 62, 699–718.
- Lachenal, A.-M., 1989. Ecologie des ostracodes du domaine Méditerranéen: application au Golfe de Gabes (Tunisie orientale). *Documents Laboratoire Geologie de Lyon* 108, 1–239.
- Locardi, E., Lombardi, G., Funicello, R., Parotto, M., 1977. The main volcanic groups of Latium (Italy): relations between structural evolution and petrogenesis. *Geologica Romana* 15, 279–300.
- Lourens, L.J., Hilgen, F.J., Raffi, I., Vergnaud-Grazzini, C., 1996. Early Pleistocene chronology of the Vrica section (Calabria, Italy). *Paleoceanography* 11, 797–812.
- Lourens, L.J., Hilgen, F.J., Raffi, I., 1998. Base of large Gephyrocapsa and astronomical calibration of Early Pleistocene sapropels in Site 967 and Hole 969D: solving the chronology of the Vrica section (Calabria, Italy). In: Robertson, A.H.F., Emeis, K.-C., Richter, C., Camerlenghi, A. (Eds.), *Proceedings of the Ocean Drilling Program, Scientific Results*, 160, pp. 191–197.
- Lourens, L.J., Hilgen, F.J., Shackleton, N.J., Laskar, J., Wilson, D., 2004. The Neogene Period. In: Gradstein, F.M., Ogg, J.G., Smith, A.G. (Eds.), *A Geological Time Scale 2004*. Cambridge University Press, Cambridge, pp. 409–440.
- Malatesta, A., (Ed.) 1978. *Torre in Pietra – Roma. Quaternaria* 20, 203–577.
- Malatesta, A., Zarlenga, F., 1986. Nothern guests in the Pleistocene Mediterranean Sea. *Geologica Romana* 25, 54–91.
- Marra, F., 1993. *Stratigrafia e assetto geologico-strutturale dell'area romana tra il Tevere e il Rio Galeria*. *Geologica Romana* 29, 515–535.
- Marra, F., Carboni, M.G., Di Bella, L., Faccenna, C., Funicello, R., Rosa, C., 1995. Il substrato plio-pleistocenico nell'area romana. *Bollettino della Società Geologica Italiana* 114, 195–214.
- Marra, F., Rosa, C., De Rita, D., Funicello, R., 1998. Stratigraphic and tectonic features of the Middle Pleistocene sedimentary and volcanic deposits in the area of Rome (Italy). *Quaternary International* 47/48, 51–63.
- Mattei, M., Cipollari, P., Cosentino, D., Argentieri, A., Rossetti, F., Speranza, F., Di Bella, L., 2002. The Miocene tectono-sedimentary evolution of the southern Tyrrhenian Sea: stratigraphy, structural and palaeomagnetic data from the on-shore Amantea basin (Calabrian Arc, Italy). *Basin Research* 14, 147–168.
- McFadden, P.L., 1990. A new fold test for paleomagnetic studies. *Geophysical Journal International* 103, 163–169.
- Meisch, C., 2000. *Freshwater Ostracoda of Western and Central Europe*. Spektrum Akademischer Verlag, Berlin, pp. 1–522.
- Milli, S., 1997. Depositional setting and high-frequency sequence stratigraphy of the Middle-Upper Pleistocene to Holocene deposits of the Roman Basin. *Geologica Romana* 33, 99–136.
- Montone, P., Amato, A., Chiarabba, C., Buonasorte, G., Fiordelisi, A., 1995. Evidence of active extension in Quaternary volcanoes of Central Italy from breakout analysis and seismicity. *Geophysical Research Letters* 22, 1909–1912.
- Murray, J.W., 1991. *Ecology and Paleoecology of Benthic Foraminifera*, 397 pp., Longman Scientific & Technical.
- Neale, J.W., 1988. Ostracods and Palaeosalinity reconstruction. In: De Deckker, P., Colin, J.P., Peypouquet, J.P. (Eds.), *Ostracoda in the Earth Science*. Elsevier, Amsterdam, pp. 125–155.
- Pérès, J.M., 1982. Zonation. In: Kinne, O. (Ed.), *Marine Ecology, Ocean Management*, 5. John Wiley & Sons, pp. 9–45.
- Pillans, B., Naisb, T., 2004. Defining the Quaternary. *Quaternary Science Review* 23, 2271–2282.
- Ponzi, G., 1872. *Del bacino di Roma e sua natura*. Regia Tipografia, 51 pp., 1 carta geologica.
- Ponzi, G., 1875. *Sui Monti Mario e Vaticano e del loro sollevamento*. *Atti della Regia Accademia dei Lincei* 2, 545–556.
- Raffi, I., 2002. Revision of the early-middle Pleistocene calcareous nanofossil biochronology (1.75–0.85 Ma). *Marine Micropaleontology* 45, 25–55.

- Raffi, I., Backman, J., Rio, D., Shackleton, N.J., 1993. Plio-Pleistocene nannofossil biostratigraphy and calibration to oxygen isotope stratigraphies from Deep Sea Drilling Project Site 607 and Ocean Drilling Program Site 677. *Paleoceanography* 8, 387–408.
- Raffi, I., Backman, J., Fornaciari, E., Pälike, H., Rio, D., Lourens, L., Hilgen, F., 2006. A review of calcareous nannofossil astrobiochronology encompassing the past 25 million years. *Quaternary Science Reviews* 25, 3113–3137.
- Rio, D., Raffi, I., Villa, G., 1990. Pliocene–Pleistocene calcareous nannofossil distribution in the western Mediterranean. In: Kastens, K.A., Mascle, J., et al. (Eds.), *Proceedings of the Ocean Drilling Program, Scientific Results*, 107, pp. 513–533.
- Ruddiman, W.F., Raymo, M., McIntyre, A., 1986. Matuyama 41,000-year cycles: North Atlantic Ocean and Northern Hemisphere ice sheets. *Earth and Planetary Science Letters* 80, 117–129.
- Ruggieri, G., 1954. La limite entre Pliocène et Quaternaire dans la série Plio-Pléistocène du Santerno. *Congrès Géologique International, Comptes Rendus de XIX Session, Alger 1952*. Volume 15: 235–240.
- Ruggieri, G., 1980. Sulla distribuzione stratigrafica di alcuni Ostracodi nel Pleistocene italiano. *Bollettino della Società Paleontologica Italiana* 19 (1), 127–135.
- Salvini, F., 2004. Structural data integrated system analyzer software (DAISY 3.0). Dipartimento di Scienze Geologiche, Università degli Studi Roma Tre, Rome, Italy.
- Sartori, R., 1990. The main results of ODP Leg 107 in the frame of Neogene to Recent geology of Perityrrhenian areas. In: Kastens, K.A., Mascle, J., et al. (Eds.), *Proceedings ODP, Scientific Results*, 107, pp. 715–730.
- Sartori, R., Torelli, L., Zitellini, N., Carrara, G., Magaldi, M., Mussoni, P., 2004. Crustal features along a W-E Tyrrhenian transect from Sardinia to Campania margins (Central Mediterranean). *Tectonophysics* 383, 171–192.
- Selli, R., 1954. La limite Plio-Pléistocène dans les environs d'Ancona (Marche). *Congrès Géologique International, Comptes Rendus de XIX Session, Alger 1952*. Volume 15: 241–247.
- Selli, R., Accorsi, C.A., Bandini Mazzanti, M., Bertolani Marchetti, D., Bigazzi, G., Bonadonna, F.G., Borsetti, A.M., Cati, F., Colalongo, M.L., D'Onofrio, S., Landini, W., Menesini, E., Mezzetti, R., Pasini, G., Savelli, C., Tampieri, R., 1977. The Vrica section (Calabria-Italy). A potential Neogene–Quaternary Boundary Stratotype. *Giornale di Geologia* 41, 181–204.
- Serri, G., Innocenti, F., Manetti, P., 1993. Geochemical and petrological evidence of the subduction of delaminated Adriatic continental lithosphere in the genesis of the Neogene–Quaternary magmatism of central Italy. *Tectonophysics* 223, 117–147.
- Shackleton, N.J., 1995. New Data on the Evolution of Pliocene Climatic Variability. In: Vrba, E.S., Denton, G.H., Partridge, T.C., Burckle, L.H. (Eds.), *Paleoclimate and Evolution, with Emphasis on Human Origins*. Yale University Press, pp. 242–248.
- Shackleton, N.J., Berger, A., Peltier, W.R., 1990. An alternative astronomical calibration of the lower Pleistocene timescale based on ODP Site 677. *Transactions of the Royal Society of Edinburgh Earth Sciences* 81, 251–261.
- Sgarrella, F., Moncharmont-Zei, M., 1993. Benthic Foraminifera of the Gulf of Naples (Italy): systematics and autoecology. *Bollettino Società Paleontologica Italiana* 32 (2), 145–264.
- Sprovieri, R., 1992. Mediterranean Pliocene biochronology: an high resolution record based on quantitative planktonic foraminifera distribution. *Rivista Italiana di Paleontologia e Stratigrafia* 98, 61–100.
- Sprovieri, R., 1993. Pliocene–Early Pleistocene astronomically forced planktonic foraminifera abundance fluctuations and chronology of Mediterranean calcareous plankton bioevents. *Rivista Italiana di Paleontologia e Stratigrafia* 99, 371–414.
- Tellini, A., 1893. *Carta geologica dei dintorni di Roma. Regione alla destra del Tevere*. Cromolit. Danesi, Roma.
- Verri, A., 1915. *Cenni spiegativi della Carta Geologica di Roma pubblicata dal Regio Ufficio Geologico su rilevamento del generale A. Verri*. Novara, Istituto Geografico De Agostini, Novara, pp. 156.
- Wei, W., 1993. Calibration of upper Pliocene–lower Pleistocene nannofossil events with oxygen isotope stratigraphy. *Paleoceanography* 8, 85–99.
- Williams, M., Dunkerley, D., De Deckker, P., Kershaw, P., Chappell, J., 1998. *Quaternary Environments*, 329 pp. Arnold, London.